

H. Chung, W. Si, and M. Dudley (SUNY Stony Brook), D. F. Bliss (Rome Laboratory, AFB), and A. Maniatty (RPI)

Numerous slip bands nucleated from the periphery of the crystal were observed. The diffuse contrast in the slip bands and in their surrounding crystal volume revealed in most of reflections is due to the long-range strains associated with a high density of dislocations piling up on their slip planes. A judicious choice of proper projection and diffraction conditions enabled individual dislocations within a slip band to be clearly resolved. Figure 1 comprises transmission X-ray topographs recorded from a slip band showing the contrast variations of slip dislocations in different reflections. It is worth noting that individual dislocations are clearly visible in both (111) and (040) reflections, while only faint contrast associated with the intersection of the slip band on the X-ray exit surface can be discerned in both (11 $\bar{1}$) and (400) reflections. The dislocation Burgers vector b can, therefore, be determined by using the $g \cdot b = 0$ criterion, where g is the diffraction vector. The slip plane can also be determined by analyzing the projected direction and length of slip dislocations in different reflections. This slip band is, therefore, characterized to belong to the [011]/(111) slip system. Systematic characterization of all of the slip dislocations in this sample reveals that nine of the twelve possible $\langle 110 \rangle / \{111\}$ slip systems are activated at different stages of the growth process. Since slip processes were initiated from regions of stress concentration, studies of the spatial configuration of slip bands and the activation of slip systems in the as-grown crystal enable one to understand the relationship between the thermal conditions used and the crystalline perfection of the as grown crystals and provides useful information on thermal stress modeling.

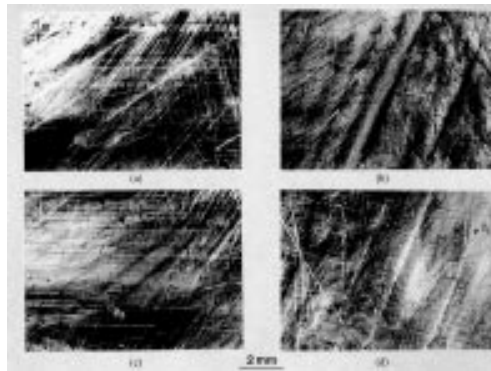


Figure 1.

* Work performed on the Stony Brook Synchrotron Topography Facility, Beamline X-19C, and supported by ARPA/AFOSR Consortium of Crystal Growth Research under Contract No. F496209510407.